

“Accurately Characterizing Hard Nonlinear Behavior of Microwave Components with the Nonlinear Network Measurement System: Introducing ‘Nonlinear Scattering Functions’”

D. Schreurs, T. Visan, S. Vandenberghe, H. van Meer, K. van der Zanden, B. Nauwelaers

*Proceedings of the 5th International Workshop on Integrated Nonlinear Microwave and Millimeterwave Circuits*, pp. 17-26, Duisburg (Germany), October 1998.

**© Copyright statement 1998, 2000 Agilent Technologies.**

Reproduced from <http://www.agilent.com/find/lsna> with permission, courtesy of Agilent Technologies, Inc.

# **Accurately Characterizing Hard Nonlinear Behavior of Microwave Components with the Nonlinear Network Measurement System: Introducing “Nonlinear Scattering Functions”**

**Jan Verspecht and Patrick Van Esch**

Hewlett-Packard Network Measurement and Description Group  
VUB-ELEC, Pleinlaan 2, 1050 Brussels, Belgium  
tel. 32-2-629.2886, fax 32-2-629.2850, email janv@belgium.hp.com

## **ABSTRACT**

*This paper describes an original way of dealing with the measuring and modeling of microwave transistor nonlinear behavior. Although generalizations are possible, the method described in this particular paper deals with transistor behavior under a large signal one-tone excitation, with arbitrary impedance terminations for the fundamental and the harmonics. First the mathematical theory of the “nonlinear scattering functions” is described. Next the measurement set-up and the actual extraction of the model parameters is highlighted. Finally the model is implemented in a commercial harmonic balance simulator. Using the simulator, model verification is performed by comparing measured and modeled behavior.*

## **INTRODUCTION**

There is a growing number of applications relying heavily on microwave technology: GSM, CDMA cellular phone, Local Multipoint Distribution Service, Japanese PCS and PDC, W-CDMA, Wireless Local Loop,... The design of the power amplifiers used in these systems is often one of the toughest problems to solve. Powerful CAD tools potentially save a lot of time. It is important, however, to be aware that these simulators can only be as accurate as the mathematical models that are used. As a consequence a lot of time is spent on constructing good models for the components used. Especially constructing models that can accurately describe the large-signal hard-nonlinear behavior of power transistors is far from trivial. The state-of-the-art is to use technology dependent analytical models (e.g. Curtice Cubic, Materka, Statz, Tajima,...) or more general “small signal measurement based” models like the HP-Root model [1]. Despite the fact that a lot of effort goes into building models for power transistors, the result is often not accurate enough to satisfy the designer. In this case time consuming loadpull measurements are being used (often these loadpull measurements need to be iterated a few times during the design cycle).

In this work another modeling approach is proposed, based upon the use of a black-box frequency domain model. The method is called “nonlinear scattering functions” and can be considered as an extension of “scattering parameters” into hard nonlinear behavior. The model can accurately simulate the behavior of a power transistor under large-signal one-tone excitation at the input, with any arbitrary impedances present at the output (fundamental and all harmonics). The model parameters are extracted based upon a relatively small set of measurements performed with an experimental loadpull set-up build around a “Nonlinear Network Measurement System” [2]. These measurements are actually a combination of passive and active harmonic loadpull measurements.

There are mainly two reasons why one can expect this approach to be more simple and accurate. Firstly one has the advantage that the model parameters are directly extracted from large signal

loadpull measurements, which are very close to the actual working conditions of the device. This implies that the behavior of the model in the simulator will be consistent with the measured harmonic loadpull behavior. Classical modeling approaches are based upon many small signal and DC measurements, which are far from the actual operating conditions. This often results in inconsistency between measured and modeled loadpull behavior.

Secondly all parasitic effects are automatically included in the black-box model, while all parasitic effects have to be explicitly identified with the other models. This makes the “nonlinear scattering functions” really technology independent. A drawback of the method is of course that the model will only be valid for one-tone excitation, with a frequency corresponding to the frequency used to extract the model.

## MATHEMATICAL THEORY

### Mathematical notations

Extending the concept of “scattering-parameters” [3] in order to describe nonlinear behavior is not trivial. One needs to go back to the basics. “Scattering parameters” are called this way because they relate incident and reflected (or scattered) travelling voltage waves at the signal ports, thereby completely describing the behavior of a linear microwave device. The “nonlinear scattering functions” have the same purpose: relating incident and reflected travelling voltage waves. Some necessary mathematical notations and concepts are introduced in the following.

Incident voltage waves will be denoted by the symbol “a” and reflected voltage waves will be denoted by the symbol “b”. In many cases travelling voltage waves (and the corresponding s-parameters) are defined in a characteristic impedance of 50 Ohm. When dealing with nonlinear behavior, however, it may be convenient to use different characteristic impedances. The characteristic impedance used for the definition of the waves will be indicated between brackets as a subscript. When the impedance is not indicated it is assumed to be 50 Ohm, or that the value is irrelevant for the given formula. The relationship between voltage “v”, current “i” (defined as being positive when flowing into the device-under-test, called DUT, signal port) and the travelling voltage waves is given by

$$a_{(Z)} = \frac{v + Zi}{2} \quad b_{(Z)} = \frac{v - Zi}{2} . \quad (1)$$

As mentioned in the introduction, we will describe the device behavior under sinusoidal (one-tone) excitation. Excluding subharmonic and chaotic behavior, all signals appearing at the DUT ports will have the same periodicity (= the reciprocal of the fundamental frequency). The periodic signals will be described by their complex Fourier series coefficients, which are commonly called the “spectral components” of the signal. Each “spectral component” has an associated “harmonic index”, which denotes the ratio between the associated frequency and the fundamental. The “harmonic index” will be indicated by the last subscript. An “harmonic index” equal to zero corresponds to DC. The first subscript indicates the respective DUT signal port. Port 1 will typically correspond to the input (gate, base) and port 2 with the output (drain, collector) of the DUT. Some examples:

- $a_{(10)21}$  refers to fundamental of the incident voltage wave at port 2, defined with a characteristic impedance of 10 Ohm.
- $b_{13}$  refers to the third harmonic (with frequency equal to 3 times the fundamental frequency) at port 1, defined with a characteristic impedance of 50 Ohm.

## The black-box model

Conceptually, writing down the black-box model equation is trivial. First thing to do is to “phase normalize” all signals by applying a time delay (applying a phase shift to the spectral components proportional to the harmonic index) such that  $a_{11}$  has zero phase. This way all spectral component phases are uniquely defined. This is done as follows:

$$\begin{cases} a_{kp} = a_{kp}^{NN} \left( \frac{a_{11}^{NN}}{|a_{11}^{NN}|} \right)^{-p} \\ b_{kp} = b_{kp}^{NN} \left( \frac{a_{11}^{NN}}{|a_{11}^{NN}|} \right)^{-p} \end{cases} \quad \forall k, p, \text{ with superscript “NN” denoting “not normalized”}. \quad (2)$$

One can then simply write

$$b_{kp} = S_{kp}(\text{Re}(a_{11}), \text{Re}(a_{12}), \text{Im}(a_{12}), \text{Re}(a_{13}), \dots, \text{Re}(a_{21}), \dots). \quad (3)$$

This equation simply states that the scattered voltage wave spectral components are complex functions of the real and imaginary parts of all the incident voltage wave spectral components. The functions “ $S_{kp}$ ” are called the “nonlinear scattering functions”. Note that  $\text{Im}(a_{11})$  does not appear in the equation since this value is always zero because of the phase normalization. The modeling problem is now transformed in identifying the functions  $S_{kp}$ , for all scattered spectral components. In practice it will be sufficient to consider a limited number of harmonics (including up to the 4th harmonic has been enough for all practical cases investigated until now).

Generally speaking identifying the functions  $S_{kp}$  would imply the identification of a set of multidimensional nonlinear functions, which is practically very hard to do. In many cases, however, signal conditions are such that the functions  $S_{kp}$  can be simplified. For a power amplifier with one dominant tone at the input, all harmonic signals will be relatively small compared to the fundamental signals. It is then possible to expand the functions  $S_{kp}$  into a MacLaurin series [7] for all harmonic components (excluding the fundamental components at both signal ports). This results in

$$b_{kp} = F_{kp} + \sum_{\substack{i=1,2 \\ j=2,\dots,N}} G_{kpij} \text{Re}(a_{ij}) + \sum_{\substack{i=1,2 \\ j=2,\dots,N}} H_{kpij} \text{Im}(a_{ij}). \quad (4)$$

In this equation  $N$  represents the highest harmonic index considered.  $F_{kp}$ ,  $G_{kpij}$  and  $H_{kpij}$  are functions of  $\text{Re}(a_{11})$ ,  $\text{Re}(a_{21})$  and  $\text{Im}(a_{21})$  (= fundamental components), they are given by

$$F_{kp}(\text{Re}(a_{11}), \text{Re}(a_{21}), \text{Im}(a_{21})) = S_{kp}(\text{Re}(a_{11}), \text{Re}(a_{21}), \text{Im}(a_{21}), 0, 0, \dots)$$

$$G_{kpij}(\text{Re}(a_{11}), \text{Re}(a_{21}), \text{Im}(a_{21})) = \left. \frac{\partial S_{kp}}{\partial \text{Re}(a_{ij})} \right|_{a_{rs}=0; \forall r, \forall s > 1}. \quad (5)$$

$$H_{kpij}(\text{Re}(a_{11}), \text{Re}(a_{21}), \text{Im}(a_{21})) = \left. \frac{\partial S_{kp}}{\partial \text{Im}(a_{ij})} \right|_{a_{rs}=0; \forall r, \forall s > 1}$$

This reduces the problem to fitting a set of three dimensional functions. A practical example of this approach, based on harmonic balance simulations, is given in [4]. The three dimensional fitter used in [4] is a simple linear grid interpolator.

As will be illustrated by the actual measurements, it is possible to further simplify (5) without significant reduction of the application domain. The idea is that power amplifier designers are particularly interested in the transistor loadpull behavior in a limited area of the Smith chart. This area corresponds to a limited range of output impedances, typically around a certain value  $Z$ . When  $Z$  is present at port 2 it is obvious that  $a_{(Z)21}$  is equal to zero (by definition, cf. (1)). For impedances deviating a little from  $Z$ ,  $a_{(Z)21}$  will be small enough in order to linearize  $S_{kp}$  also in the variables  $\text{Re}(a_{(Z)21})$  and  $\text{Im}(a_{(Z)21})$  (the fundamental at signal port 2). Practical experience learns that the resulting model is valid for output impedances ranging from 0.5 times  $Z$  to 2  $Z$ . The modeling approach as described by (5) is only valid for fixed biasing settings. The dependencies on the biasing can simply be included in the model as extra nonlinear parameters. This finally results in the black-box model described by

$$b_{kp} = F_{kp} + G_{kp21} \text{Re}(a_{(Z)21}) + H_{kp21} \text{Im}(a_{(Z)21}) + \sum_{\substack{i=1,2 \\ j=2,\dots,N}} G_{kpij} \text{Re}(a_{ij}) + \sum_{\substack{i=1,2 \\ j=2,\dots,N}} H_{kpij} \text{Im}(a_{ij}), \quad (6)$$

with all  $F$ ,  $G$  and  $H$  being complex functions of  $\text{Re}(a_{11})$ , and the independent bias settings. These bias settings are typically base current and collector voltage (bipolar technology), or gate voltage and drain voltage (FET technology).

Several approaches are possible in order to fit these  $F$ ,  $G$  and  $H$  functions with three real arguments. The simplest approach is to use straight interpolation between measured points, lying on a three dimensional grid, as applied in [4]. Since it is not trivial to measure exactly on a grid, we looked for fitters allowing to get input data on random samples. Good results were obtained with feedforward artificial neural nets (ANN) ([5] and [6]).

#### On the artificial neural nets used to model the “nonlinear scattering functions”

A lot of literature is available on using artificial neural nets as multidimensional function fitters. A short introduction, focused on the one particular type of neural nets we used, is given in what follows.

Suppose one wants to model a set of  $M$  output functions (denoted by “ $y_i$ ”) having  $R$  inputs (denoted by “ $x_i$ ”), and suppose one knows that there is quite some correlation in the behavior of the  $M$  different functions. For the type of neural net we use, the fitted function then has the following mathematical form:

$$y_i = \sum_{j=1}^Q W_{ij} \text{sigm}(h_j) + \alpha_i, \quad \text{with} \quad (7)$$

$$h_j = \sum_{k=1}^R V_{jk} x_k + \beta_j. \quad (8)$$

In (7) and (8), model parameters are the matrices  $W_{ij}$  and  $V_{jk}$  and the vectors  $\alpha_i$  and  $\beta_j$ . Note that the vector  $h_j$  (containing  $Q$  elements) is only used as an intermediate variable. The function “sigm” is the so-called sigmoid function, defined as

$$\text{sigm}(x) = \frac{1}{1 + e^{-x}}. \quad (9)$$

This function is often used for constructing ANNs. It is a very smooth function, going asymptotically to 0 for negative values, and to 1 for positive values. The fact that the class of functions described by (7) and (8) can fit any smooth multidimensional function can be explained

as follows.

The output function is written as a linear combination, with offset, of the functions  $\text{sigm}(h_j)$ , being equal to

$$\text{sigm}\left(\sum_{k=1}^R V_{jk}x_k + \beta_j\right). \quad (10)$$

This function is constant on all hyperplanes (a plane with dimension R-1) parallel with the one described by

$$\sum_{k=1}^R V_{jk}x_k = 0. \quad (11)$$

As such, this function divides the R-dimensional input spaces into two regions, separated by a hyperplane, being equal to 1 in one region, and being equal to 0 in the other region, with a smooth transition between the two regions (cf. (9)). It is not hard to imagine that about every smooth function can be approximated by a superposition (with offset) of such functions. Rigorous proves exist in literature.

An ANN is often represented by a schematic, as shown in Fig. 1. Each point in the schematic is called a node, the nodes in the middle are called the hidden layer, the vectors  $\alpha_i$  and  $\beta_j$  are called the node biases and the matrices  $W_{ij}$  and  $V_{jk}$  are called the weights of the node connections. The problem is then to start from a random set of measured input values and associated output values, and to calculate values of the matrices  $W_{ij}$  and  $V_{jk}$  and the vectors  $\alpha_i$  and  $\beta_j$  resulting in a good correspondence between measured and modeled data. In order to do this we used a Levenberg-Marquardt algorithm [8]. Further optimization is performed by a pruning technique called ‘‘Optimal Brain Surgeon’’, described in [9]. The pruning technique selectively removes node connections, thereby simplifying the model. The algorithm is implemented using the so-called ‘‘Neural Network Based System Identification Toolbox’’ of Magnus Nørsgaard [5].

For our application, one ANN is trained (= fitted) for each  $F_{kp}$  and each set  $(G_{kp1j}, G_{kp2j}, H_{kp1j}, H_{kp2j})$ . So there are two classes of ANN’s: the ones describing the  $F_{kp}$ ’s, having three input nodes ( $\text{Re}(a_{11})$  and the two bias settings) and two output nodes (real and imaginary part of  $F_{kp}$ ), and the ones describing the G and H’s, having three input nodes and 8 output nodes (real and imaginary parts of  $G_{kp1j}, G_{kp2j}, H_{kp1j}, H_{kp2j}$ ). Although other arrangements are certainly possible, the one chosen is a good practical compromise between model complexity and ease of fitting.

## MEASUREMENT SET-UP AND MODEL EXTRACTION

In order to identify the model, a measurement set-up is needed allowing to apply sufficient excitation signals to the DUT, and to accurately measure the spectral components (both a’s and b’s). The set-up realized is depicted in Fig. 4. The NNMS system, an advanced version of the system described in [2], automatically performs the accurate measurement of all spectral components needed for the model (system bandwidth at present is 20 GHz). The bias is controlled and accurately measured by an HP-4142B semiconductor parameter analyzer. The system contains two microwave synthesizers. ‘‘Synth 1’’, connected to a ZHL-42 power amplifier, generates the  $a_{11}$  signal. ‘‘Synth 2’’, connected to a switch, duplexers and power amplifiers, allows the generation of all other incident spectral components (one at the time). The tuner determines the fundamental impedance range to be covered by the model. For this particular case Z equals about 10 Ohm. When the synthesizer is set to the fundamental frequency and its output is directed towards port 2 active loadpull occurs, thereby synthesizing impedances deviating from the one set

by the tuner. The impedance range covered is about 5 Ohms to 20 Ohms.

The actual model extraction of a DUT is illustrated by example. The example DUT is a silicon BJT power transistor. First the tuner is set such that the fundamental impedance (frequency used was 1.88 GHz) seen by the collector is lying within the interesting part of the Smith chart, in this case about 10 Ohm. Next the values of all F, G and H's under consideration (6) are determined at a random set of "large signal settings" within a certain range. The "large signal settings" are the amplitude of  $a_{11}$ , and the independent biasing parameters: base current and collector voltage. 500 randomly chosen settings were used. The peak-amplitude of  $a_{11}$  ranged from 0.5 V to 5.7 V, base current ranged from 0.12 mA to 6 mA, and collector voltage from 2 V to 5 V. Once the value of F, G and H at all sampled "large signal settings" points are measured (this will be explained in the next paragraph), a set of ANN's is trained in order to fit the data.

The values of F, G and H, at one particular setting of  $a_{11}$ , base current and collector voltage, are measured by keeping the "large signal settings" constant while sending small signal deviations  $a_{12}$ ,  $a_{13}$ ,  $a_{14}$ ,  $a_{(10)21}$ ,  $a_{22}$ ,  $a_{23}$  and  $a_{24}$  towards the DUT, and measuring all a's and b's under consideration. These small signal deviations are generated by "synth 2" (Fig. 4). Six realizations of each deviation are performed, each time randomizing the phase relationship between the "synth 1" fundamental signal and the signal of "synth 2". The values for all F, G and H's for that particular "large signal setting" are found by performing a least-squares-error fit on the measured data. For all 500 "large signal settings" this implies a total of 21.000 measurements, which takes about 4 hours.

Fig. 2 gives an idea about the behavior of the "nonlinear scattering functions" by plotting the magnitude of  $F_{21}$  versus base current and  $\text{Re}(a_{11})$ , with a constant collector voltage of 4.5 V. Note that  $F_{21}$  can be interpreted as the value of  $b_{(10)21}$  (this is the fundamental output) with all  $a_{jk}$  equal to zero (except of course the stimulus  $a_{11}$ ). This corresponds to a 50 Ohm load seen by all harmonics and a 10 Ohm load seen by the fundamental at the output. One notes that the function is very smooth, being very small for zero biasing current, and increasing for increasing values of base current and stimulus  $a_{11}$ , as one can expect.

Harmonic distortion information is also present in the model. This is illustrated by Fig. 3. Under the same matching conditions as those used in Fig. 2, all harmonic distortion information (in this example up to the third harmonic) is present in  $F_{21}$ ,  $F_{22}$  and  $F_{23}$ , evaluated at a specific bias point. Note that the model tends to behave abnormal for small input powers, in the sense that the amplitude does not roll off with the expected constant slope. This is an artifact of the neural net, which, by construction, does not respect the typical polynomial asymptotic behavior if  $a_{11}$  goes to zero (cf. Volterra theory [10]). Although this fact should not be a problem for typical power amplifier design, designed to work at rather high input power, progress is being made in getting correct asymptotic model behavior, combining VIOMAP techniques [11] with neural nets.

## MODEL VERIFICATION

The model extracted was integrated into an harmonic balance simulator and comparisons were made between actual measured and modeled data. One example of this is given by Fig. 5. The figure represents an overlay of the measured and modeled current and voltage waveforms at the transistor signal ports, for one point in the measured range. The reflection coefficient of the fundamental seen by the collector has a magnitude of 0.63, at an angle of 135 degrees. The reflection coefficients of the second, third and fourth harmonic are significant. Modeled output power is 419 mW, with a power-added-efficiency (PAE) of 76%, while measured output power is 392 mW with a measured PAE of 71%. The model was validated in a similar way over the whole

range. The model predicts PAE and output power with acceptable accuracy in most of the validation range. It should be noted, however, that this particular model does a bad job in predicting the power absorbed at the input. This is probably due to ill-conditioning, caused by the high fundamental reflection coefficient at the base ( $a_{11}$  and  $b_{11}$  are 50 Ohm quantities). The absorbed input power is as such equal to the difference of two relatively large numbers. Expressing  $a_{11}$  and  $b_{11}$  in another carefully selected characteristic impedance can probably solve this problem.

## CONCLUSIONS

“Nonlinear scattering functions” can accurately be measured with an automated set-up containing a “Nonlinear Network Measurement System”. The corresponding model describes the behavior of the hard-nonlinear microwave component under a large-signal one-tone excitation (relatively small harmonics may be present), and can be integrated in a commercial harmonic balance simulator.

## ACKNOWLEDGEMENTS

The authors want to thank Dave Wu of Hewlett-Packard CSSD and prof. Alain Barel of the “Vrije Universiteit Brussel” for providing the necessary hardware.

## REFERENCES

- [1] “HP 85150B Microwave and RF Design Systems - Component Catalog - Vol. 4 - Microwave Library Components,” Hewlett-Packard Co., USA, 1994.
- [2] Jan Verspecht, Peter Debie, Alain Barel and Luc Martens, “Accurate On Wafer Measurement Of Phase And Amplitude Of The Spectral Components Of Incident And Scattered Voltage Waves At The Signal Ports Of A Nonlinear Microwave Device,” *Conference Record of the IEEE Microwave Theory and Techniques Symposium 1995*, Orlando, Florida, USA, pp. 1029-1032, May 1995.
- [3] K. Kurokawa, “Power Waves and the Scattering Matrix,” *IEEE Transactions on Microwave Theory and Techniques*, March 1965, pp. 194-202.
- [4] Jan Verspecht, “Black Box Modelling of Power Transistors in the Frequency Domain,” *Conference Record of the INMMC 1996 Workshop*, October 1996, Duisburg, Germany.
- [5] Magnus Nørgaard, “Neural Network Based System Identification Toolbox,” v1.1, Technical University of Denmark, 1997.
- [6] Patrick Van Esch and Jan Verspecht, “The use of Feedforward ANN in the building of the non-linear behavioural models of microwave components in the frequency domain,” *Conference Record of the International Workshop on Advanced Black-Box Techniques for Nonlinear Modeling*, Leuven, Belgium, July 1998.
- [7] “CRC - Standard Mathematical Tables”, 27th Edition, CRC Press, Inc., 1985.
- [8] C. W. Marquardt, “An algorithm for least-squares estimation of nonlinear parameters,” *SIAM J.*, Vol. 11, pp. 431-441, 1963.
- [9] B. Hassibi, D. G. Stork, “Second Order Derivatives for Network Pruning: Optimal Brain Surgeon,” *NIPS 5*, Eds. S. J. Hanson et al., Morgan Kaufmann, 1993.
- [10] M. Schetzen, “The Volterra and Wiener Theories of Nonlinear Systems,” Wiley Interscience Publications, 1980.
- [11] F. Verbeyst and M. Vanden Bossche, “VIOMAP, the s-parameter equivalent for weakly nonlinear RF and microwave devices,” *IEEE Transactions on Microwave Theory and Techniques*, Vol. 42, No. 12, pp. 2531-2535, December 1994.

Fig. 1 Schematic representation of an ANN

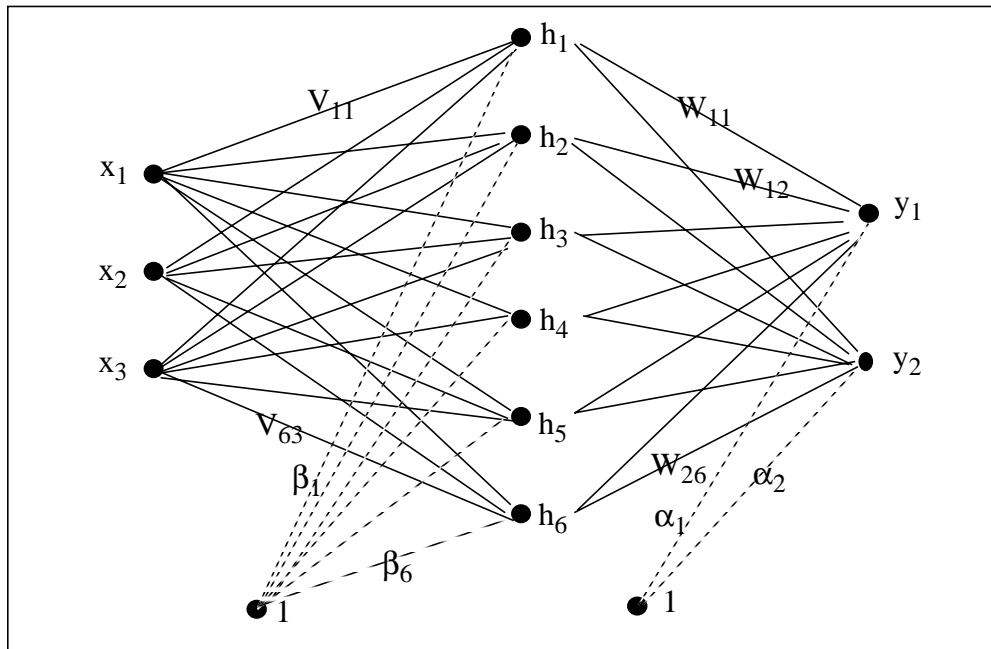


Fig. 2 Magnitude of  $F_{21}$  as a function of  $\text{Re}(a_{11})$  and  $I_{\text{base}}$ , with  $V_{\text{collector}} = 4.5 \text{ V}$

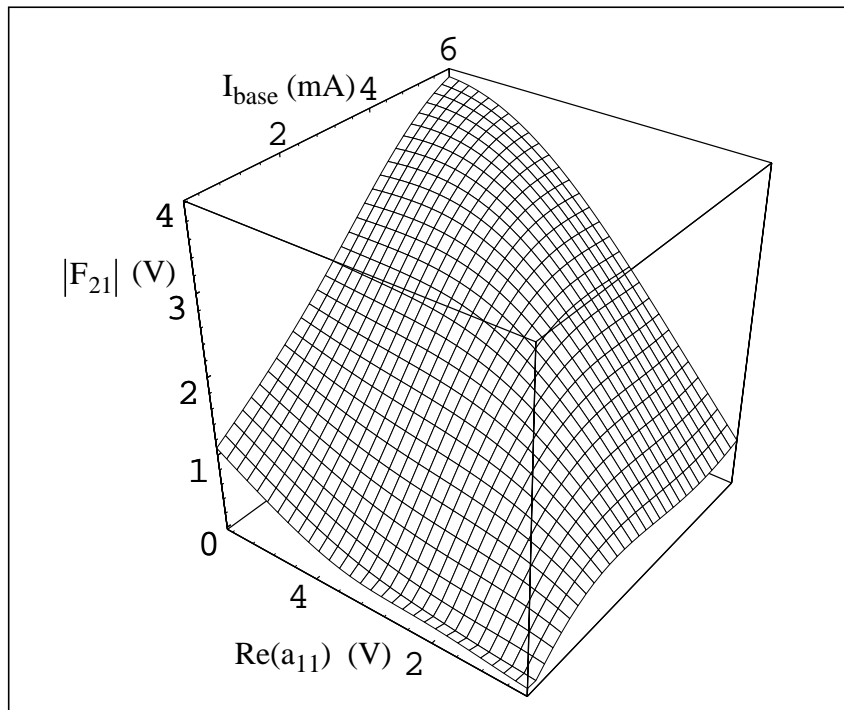


Fig. 3 Harmonic distortion analysis with  $I_{\text{base}} = 5 \text{ mA}$  and  $V_{\text{collector}} = 4.5 \text{ V}$

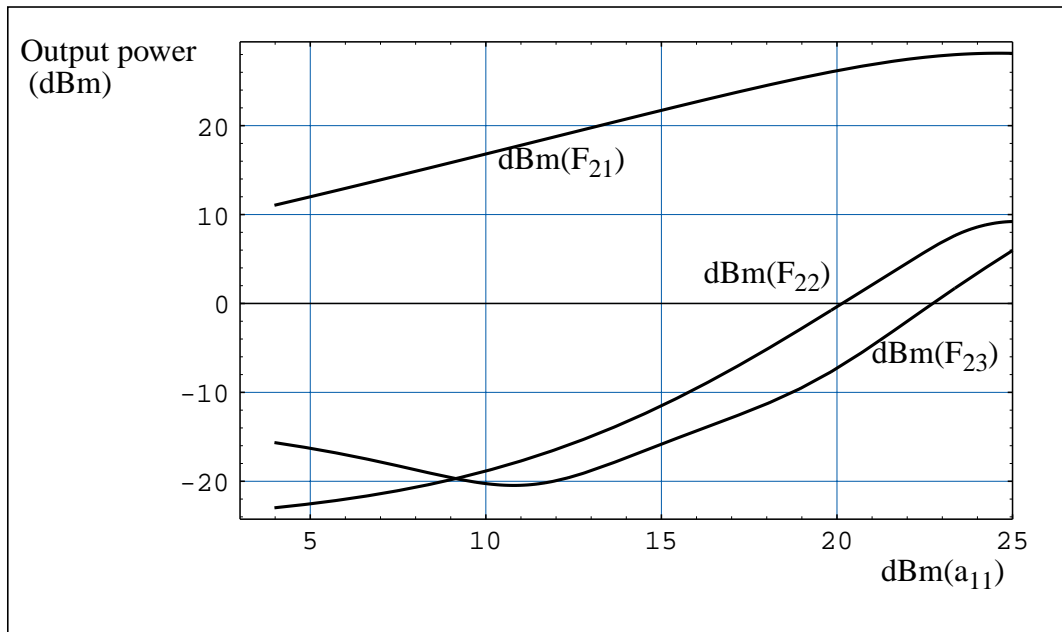


Fig. 4 Measurement set-up

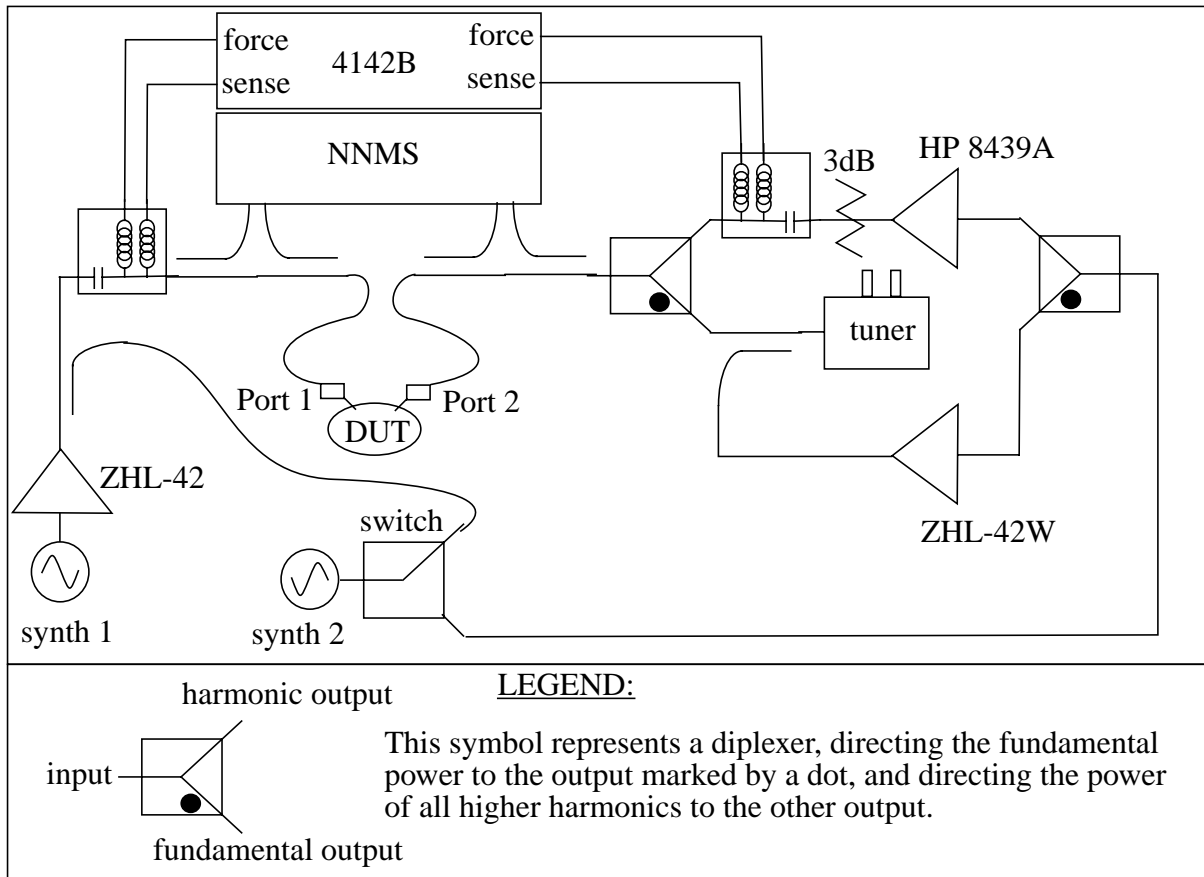


Fig. 5 Modeled and measured time domain current and voltage waveforms

